

Magnetic permeability of a diphasic flow, made of liquid gallium and iron beads

 A. Martin¹, P. Odier¹, J.-F. Pinton^{1,a}, and S. Fauve²
¹ Laboratoire de Physique^b, École Normale Supérieure, 46 Allée d'Italie, 68007 Lyon, France

² Laboratoire de Physique Statistique^c, École Normale Supérieure, 24 rue Lhomond, 75005 Paris, France

Received 6 March 2000 and Received in final form 13 July 2000

Abstract. Magnetohydrodynamics studies in laboratory experiments have long been restricted to low magnetic Reynolds number flows, mainly as a result of the very high magnetic diffusivity $\lambda = 1/\mu\sigma$ of common conducting fluids (μ is the fluid's magnetic permeability and σ its electrical conductivity). The best conductivities are found in liquid metals which have a unit magnetic permeability, relative to vacuum. We show experimentally that a suspension of solid particles with a high magnetic permeability in a liquid metal yields an effective medium that has a high electrical conductivity and an enhanced magnetic permeability. The dispersion of the beads results from the turbulent fluid motion. The range of accessible magnetic Reynolds number can be increased by a factor of as much as 4 in our experimental setup.

PACS. 47.65.+a Magnetohydrodynamics and electrohydrodynamics – 75.50.Mm Magnetic liquids – 47.55.Kf Multiphase and particle-laden flows

1 Introduction

The study of flows in fluids that have magnetic properties has led to the development of ferrohydrodynamics (FHD), with very rich applications in engineering and in the understanding of various instability phenomena [1]. Ferrofluids are usually made of colloidal suspensions of iron particle in a solvent and have a very small electrical conductivity. On the other hand, the study of flows of electrically conducting fluids, or magnetohydrodynamics (MHD), is of relevant in many physical or astrophysical situations. Important effects, such as the generation of self-excited dynamos, are expected to occur [2]. The MHD equations for the magnetic induction are:

$$\frac{\partial \mathbf{B}}{\partial t} = \mathbf{curl}(\mathbf{u} \times \mathbf{B}) + \frac{1}{\mu\sigma} \Delta \mathbf{B}, \quad \mathbf{div} \mathbf{B} = 0, \quad (1)$$

where \mathbf{u} is the velocity of the fluid, with permeability μ and conductivity σ . The relative amplitude of the induction term to the dissipative one is given by the magnetic Reynolds number

$$R_m = \mu\sigma UL, \quad (2)$$

where L and U are characteristic size and speed of the flow motion. For example dynamo action is supposed to occur when the stretching of magnetic field lines exceeds the

Joule dissipation, that is above a critical value R_m^* [2]. The search of higher R_m has led experimentalists to develop studies in high conducting liquid metals such as gallium [3] or sodium [4]. However, molten metals have a quite small kinematic viscosity ν and hence a very small magnetic Prandtl number $P_m = \mu\sigma\nu$: flows with very high kinetic Reynolds numbers must be produced to achieve even moderate magnetic Reynolds number situations. This results in a high energetic cost for the production of flows with $R_m \gtrsim \mathcal{O}(1)$. Indeed, it may be shown dimensionally, and it is confirmed experimentally [5], that the power needed to generate a turbulent flow with characteristic velocity U and volume $V = L^3$ varies as:

$$P = K\rho U^3 V^{2/3}, \quad (3)$$

where the constant K is flow dependent and ρ is the fluid's density. In other words, the magnetic Reynolds number in a given experiment depends on the flow volume and available mechanical power input as:

$$R_m = \mu\sigma \left(\frac{P}{K\rho} \right)^{1/3} V^{1/9}. \quad (4)$$

The above expression clearly shows how difficult it is to access high R_m regimes in the laboratory: an increase by even a modest factor of 2 requires an 8-fold increase in the power input or 512-fold increase in the flow volume. The only linear factors are the conductivity and the permeability. The former is optimized using liquid sodium for which appropriate technology has been made available during

^a e-mail: pinton@ens-lyon.fr

^b CNRS UMR 5672

^c CNRS UMR 8550

the development of the cooling circuits of fast breeder nuclear reactors. In this letter we show that the effective permeability of a flow can be enhanced using a binary mixture of liquid metal and magnetic solid particles.

2 Experimental setup

Our experimental set-up is schematically shown in Figure 1. Two 11 kW ac-motors are used to drive disks (radius $R = 10$ cm) at a constant frequency Ω , adjustable in the range 5 to 25 Hz. The disks are fitted with vertical blades (height equal to 5 mm) to ensure an inertial entrainment of the fluid, for which equation (3) is verified [5]. The disks are counter rotated, to enhance differential rotation which is a key feature of magnetic induction in conducting liquids [3,4].

The enclosing cylindrical vessel has an effective volume of 6 liters. It is filled with liquid gallium (density $\rho = 6.09 \times 10^3$ kg m⁻³), electrical conductivity ($\sigma = 3.68 \times 10^6$ ohm⁻¹ m⁻¹, kinematic viscosity is $\nu = 3.1 \times 10^{-7}$ m² s⁻¹). A variable volume fraction Φ of spherical iron beads (diameter $d = 6.35$ mm) is added to the gallium. The integral kinematic and magnetic Reynolds numbers of the flow are defined as: $R_e = 2\pi R^2 \Omega / \nu$ and $R_m = 2\pi \mu \sigma R^2 \Omega$. Here ν and μ are effective values of the binary gallium/iron beads mixture. In the range of flow velocities covered by our experiment, the dispersive grain pressure [6,7] homogenizes the particle distribution. The flow is strongly turbulent: R_e exceeds 10^6 . The power input by the driving disks (given by Eq. (3) with an effective density that depends on particle volume fraction $\rho = \Phi \rho_{\text{iron}} + (1 - \Phi) \rho_{\text{gallium}}$) is dissipated into heat by the turbulent motion and drained off by the cooling circuits located behind the disks. For each run at a fixed rotation rate, the flow is kept at a constant temperature $\theta \in [40, 80]$ °C. Two pairs of Helmholtz coils are set to produce an external field B_0 up to 40 gauss, either parallel or perpendicular to the rotation axis. Magnetic measurements are performed inside the vessel using directional and temperature compensated Hall probes with a Bell 9905 gaussmeter; the spatial resolution is 3 mm, with a frequency range of 50 kHz in *AC* mode or 400 Hz in *DC* mode.

3 Results

3.1 Measurement of an intrinsic magnetic Reynolds number

In order to quantify the influence of the iron beads on the magnetic properties of the binary mixture, we apply an external magnetic field and we measure the magnetic induction generated by the flow as a function of the rotation rate and the volume fraction of iron beads. We first consider the homogeneous case ($\Phi = 0$): we measure the field \mathbf{b} induced by the fluid motion in the presence of an externally applied field \mathbf{B}_0 . At low R_m , one is in a “quasistatic”

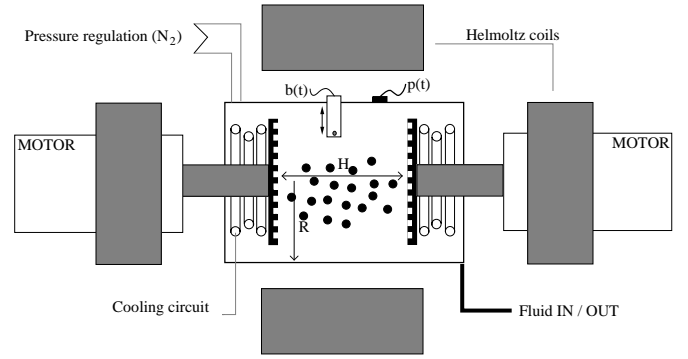


Fig. 1. Experimental set-up (not to scale). $R = 10$ cm, $H = 10$ cm. The Hall probe is located in the median plane, at a variable distance D from the rotation axis.

regime [8], where equation (1) yields to leading order:

$$\Delta \mathbf{b} \approx -\mu \sigma (\mathbf{B}_0 \cdot \nabla) \mathbf{u}. \quad (5)$$

We show in Figure 2 that b has indeed a linear variation with B_0 . The magnetic induction is mainly sensitive to changes of the flow at integral scale: in the ‘passive vector’ regime considered here, the magnetic energy falls off very rapidly at small scales – $E_B(k) \sim k^{-11/3}$, in the standard turbulence picture [3,8] – so that the large scale velocity variations give the leading contribution. One observes in Figure 2a that the induction varies smoothly with the location of the measurement. In addition, the induced field \mathbf{b} strongly depends on the anisotropy of the flow and is thus dependent on the orientations of \mathbf{b} and \mathbf{B}_0 . For example, at the location of measurement in Figure 2b (median plane, $r = 5$ cm), the transverse variation of the axial speed $\partial_x u_z$ is smaller than the differential rotation $\partial_z u_x$. This anisotropy persists as R_e increases.

Equation (5) together with the above experimental results enable us to define an *intrinsic* magnetic Reynolds number R_m^i as:

$$R_m^i = \left(\frac{\partial b}{\partial B_0} \right)_\Omega, \quad (6)$$

where the derivative is to be taken for a given flow geometry and kinetic Reynolds number, here at constant rotation rate Ω . R_m^i is thus experimentally obtained as the slope of the curves $b(B_0)$ such as shown in Figure 2b. The advantage of this definition is that the large scales velocity gradients are taken into account both in magnitude and direction in the value of R_m^i . We observe that the variations of R_m^i with R_m is linear but with different slopes depending on the orientations, as shown in Figure 2c.

Another noteworthy feature is that the intrinsic magnetic Reynolds number R_m^i is quite small: $R_m^i \sim 0.01 R_m$, see Figure 2c. This is an *a posteriori* justification of the quasistatic approximation. Note that another definition of an intrinsic magnetic Reynolds number would be: $R_m^i = \mu \sigma L' u'$, with u' the rms amplitude of velocity fluctuations and L' an effective integral scale of the flow. These quantities can be obtained from independent measurements, such as pressure fluctuations and power

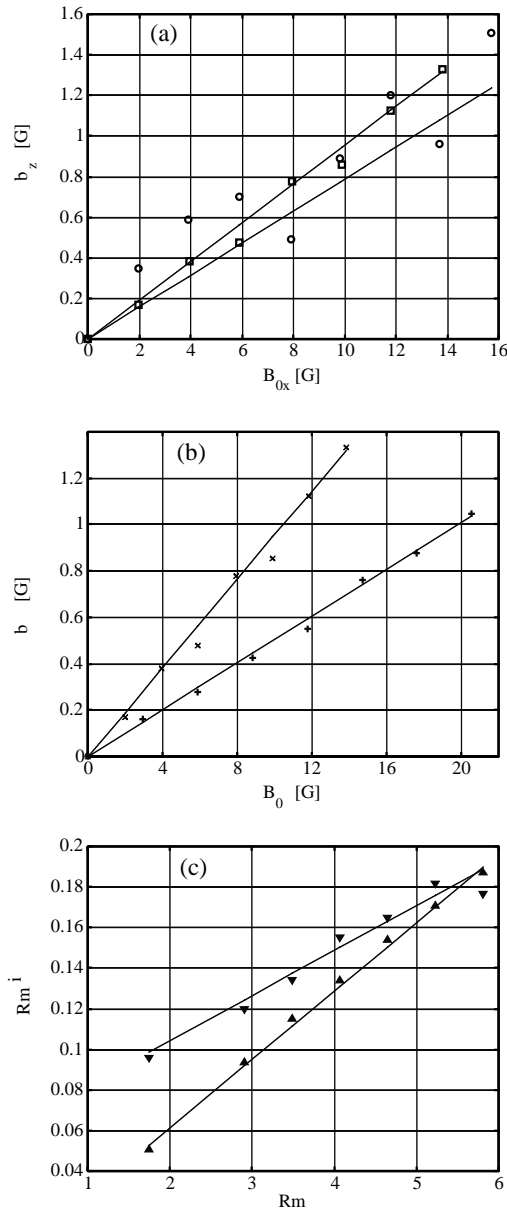


Fig. 2. Induction measurements. (a) $b_z = f(B_{0x})$ at various depth, (o): $r = 5$ cm, (\square): $r = 8$ cm, measured from the rotation axis, at $\Omega = 6$ Hz. (b) Effect of orientation: (+): $b_z = f(B_{0x})$, (\times): $b_x = f(B_{0z})$, $\Omega = 6$ Hz. (c) Variation of R_m^i with R_m . (∇): measurement of b_x , with B_{0z} applied, (\triangle): measurement of b_z , with B_{0x} applied.

consumption [5]; studies in a similar setup using water as the working fluid lead to $L' \sim 0.1L$ and $u' \sim 0.4R\Omega$, which again is consistent with our observation that there is over an order of magnitude between the calculated integral magnetic Reynolds number and the measured intrinsic one.

3.2 Influence of the iron beads

Having defined an intrinsic magnetic Reynolds number from the actual induction effects inside the flow, we can

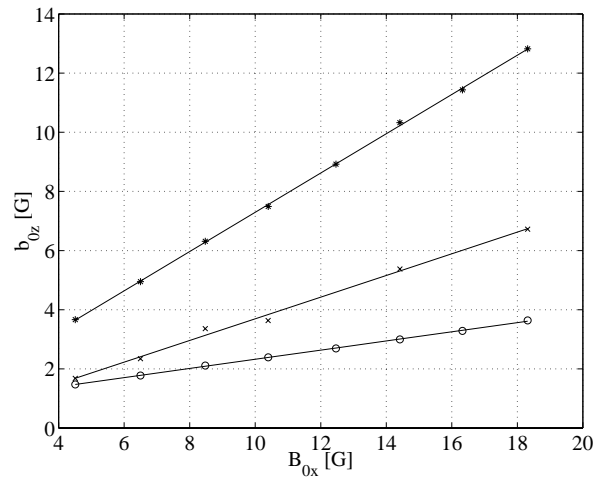


Fig. 3. Measurement of b_z induced with B_{0x} , at $\Omega = 14$ Hz. (o): homogeneous flow, (\times): bead volume fraction $\Phi = 0.3$; (*): bead volume fraction $\Phi = 0.45$.

Table 1. Gain in intrinsic magnetic Reynolds number for two bead volume fraction, as a function of the rotation rate of the disks driving the flow. Note that it is not a monotonic function of either parameter.

Ω [Hz]		10	12	14	16	18
$\frac{R_m^i(\Phi = 0.3)}{R_m^i(0)}$	(b_x, B_{0z})	4.35	4.89	4.75	4.08	–
$\frac{R_m^i(\Phi = 0.3)}{R_m^i(0)}$	(b_z, B_{0x})	2.51	2.49	2.37	–	–
$\frac{R_m^i(\Phi = 0.45)}{R_m^i(0)}$	(b_x, B_{0z})	3.61	–	3.31	–	3.00
$\frac{R_m^i(\Phi = 0.45)}{R_m^i(0)}$	(b_z, B_{0x})	4.59	–	4.29	–	4.00

study the influence of the volume fraction of iron beads on the magnetic properties of the flow. Figure 3 shows the variation of the induced field *versus* the applied field, for the homogeneous flow and for two values of particle volume fraction. It is readily observed that the presence of iron beads increases the induction effects in the flow.

At a given rotation rate of the driving disks, the ratio of the observed slopes to that of the homogeneous case yields the gain in magnetic Reynolds number. Our results for two bead volume fractions, at increasing rotation rates of the disks driving the flow are shown in Table 1. We note that the gain in magnetic Reynolds number can exceed a factor of 4, a feature that would be quite difficult to obtain by an increase of the velocity or the volume of the homogeneous flow.

Given that the electrical conductivity of the iron beads and of the liquid gallium are almost equal, it is tempting to associate these changes variations in the magnetic properties (we will come back to that assumption). Then the gain in magnetic Reynolds number is a measurement

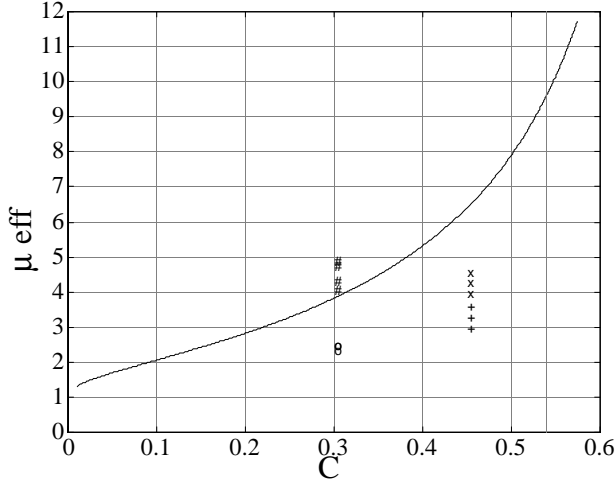


Fig. 4. Effective permeability of a gallium - iron bead mixture, from equation (9). Our measurements are: (o): b_z, B_{0x} , for $\Phi = 0.3$, (#): b_x, B_{0z} , for $\Phi = 0.3$, (x): b_z, B_{0x} , for $\Phi = 0.45$, (+): b_x, B_{0z} , for $\Phi = 0.45$. The dash-dotted line corresponds to the limit volume fraction above which the binary mixture behaves like a solid.

of the relative effective permeability of the binary mixture – $\mu_{\text{eff}} = R_m^i(\Phi)/R_m^i(0)$.

The computation of μ_{eff} is possible only in two limits: small volume fraction of beads or nearly equal magnetic permeabilities of the two phases. In our case, $\mu_b \gg 1$, and the volume fractions are rather high. We can however, give a crude estimate of μ_{eff} when the volume fraction is large, such that the mean distance, a , between the beads is small compared to their diameter, d . In that case, one expects that the field lines tend to go from one bead to one of its neighbour in order to follow regions of high magnetic permeability. We consider a closed field line \mathcal{C} of length l in the medium, and write the Ampère theorem

$$\int_{\mathcal{C}} \mathbf{H} d\ell \equiv \int_{\mathcal{C}} \frac{\mathbf{B}}{\mu_{\text{eff}}} d\ell = I. \quad (7)$$

Using the continuity of the normal component of \mathbf{B} , we get

$$\frac{d}{\mu_b} + a \simeq \frac{d+a}{\mu_{\text{eff}}}. \quad (8)$$

Using the relation between a/d and volume fraction [6], $a/d = (\Phi_0/\Phi)^{1/3} - 1$, where $\Phi_0 = \pi/3\sqrt{2} \approx 0.74$ is the maximum possible volume fraction for spheres in the bcc geometry, and taking into account that $\mu_b \gg 1$, we get

$$\mu_{\text{eff}} \simeq \frac{1}{1 - \left(\frac{\Phi}{\Phi_0}\right)^{1/3}}. \quad (9)$$

Note that in the case of low volume fraction, one cannot assume that the field line goes from one bead to its neighbour; the total length of the field line across the beads is then proportional to the volume fraction of the beads, and one get $\mu_{\text{eff}} \simeq 1 + 3\Phi$ as it should be [9].

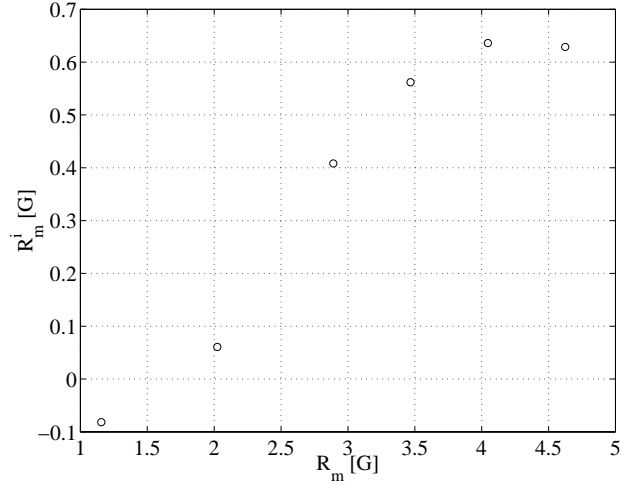


Fig. 5. Variation of the local magnetic Reynolds number with the integral one, for a bead volume fraction $\Phi = 30\%$.

We have plotted in Figure 4 the variation of the effective permeability μ_{eff} given by equation (9). We observe that it yields the right order of magnitude for the gain in magnetic Reynolds number observed in our experiment. However, the results reported in Table 1 show that the gain in magnetic Reynolds number induced by the iron beads also depends on the orientation of the measured field components and on the rotation rate of the driving disks. As the volume fraction of iron beads increases, the anisotropy in the gain in R_m^i is reduced (see Fig. 4), but the agreement with equation (9) is less satisfactory. We also observe, in contrast with Figure 2c, that the local Reynolds number R_m^i is now a non-linear function of the integral one – see Figure 5. These observations show that the mean spatial distribution of the iron beads and the velocity fields of the two phases are certainly modified both in magnitude and geometry when the disks rotation rate increase. Further investigations of the velocity topology and gradients in such a multiphase flow would be needed in order to account for the precise shape of the observed variation R_m^i vs. R_m .

4 Concluding remarks

In conclusion, we have proposed an intrinsic definition of the magnetic Reynolds number which can be easily measured by studying the response of the flow to a small external magnetic field. This can be of practical use to evaluate R_m for arbitrary flow geometries. Our results show that even a moderate volume fraction of iron beads in a liquid metal leads to a significant increase of R_m which would be difficult to achieve by increasing the velocity or the volume of the homogeneous flow.

It is a pleasure to thank Bernard Castaing for useful discussions. We are grateful to Marc Moulin for his technical assistance. We thank Rhône-Poulenc for making the gallium available to us. This work was funded by the French Ministry of Research and Education, the CNRS and the École Normale Supérieure de Lyon.

References

1. R.E. Rosensweig, *Ferrohydrodynamics* (Dover Publications, 1995).
2. W.M. Elsasser, *Am. J. Phys.* **23**, 590 (1955); P.H. Roberts, *An introduction to magnetohydrodynamics* (Longmans, 1967); H.K. Moffatt, *Magnetic field generation in electrically conducting fluids* (Cambridge U.P., 1978).
3. P. Odier, J.-F. Pinton, S. Fauve, *Phys. Rev. E* **56**, 7397 (1998).
4. A. Gailitis, O. Lielausis, S. Dementev, E. Platacis, A. Ciferons, G. Gerbeth, T. Gundrum, F. Stefani, M. Christen, H. Hänel, G. Will, *Phys. Rev. Lett.* **84**, 4365 (2000); A.B. Cawthorne, N. Peley, D. Lathrop, *Phys. Rev. E* **61**, 5287 (2000); A. Tilgner, *Phys. Earth Plan. Int.* **117**, 171 (2000).
5. N. Mordant, J.-F. Pinton, F. Chillà, *J. Phys. II France* **7**, 1 (1997); O. Cadot, Y. Couder, A. Daerr, S. Douady, A. Tsinober, *Phys. Rev. E* **56**, 427 (1997).
6. R.A. Bagnold, *Proc. Roy. Soc. A* **225**, 49 (1954).
7. J.F. Richardson, Zaki, in *Fluidization*, edited by J.F. Davidson, D. Harrison (Academic Press London, 1971); O. Molerus, *Principles of flows in disperse systems* (Chapman & Hall, 1993).
8. H.K. Moffatt, *J. Fluid Mech.* **11**, 625 (1961); G.S. Golitsyn, *Sov. Phys. Dokl.* **5**, 536 (1960).
9. A similar calculation for the electric permittivity in the low volume fraction limit can be found in: L.D. Landau, E.M. Lifshitz, *Electrodynamics of continuous media* (Pergamon Press, 1987).